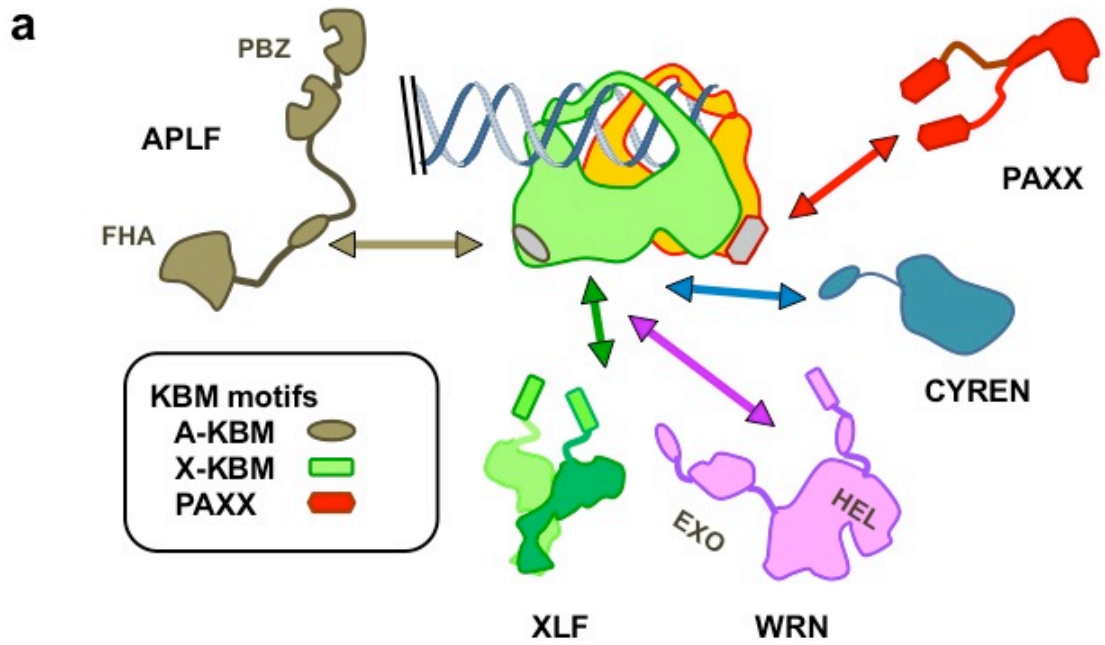
a
PBZ
APLF
FHA
PAXX
CYREN
KBM motifs
A-KBM
X-KBM
PAXX
EXO
HEL
XLF
WRN

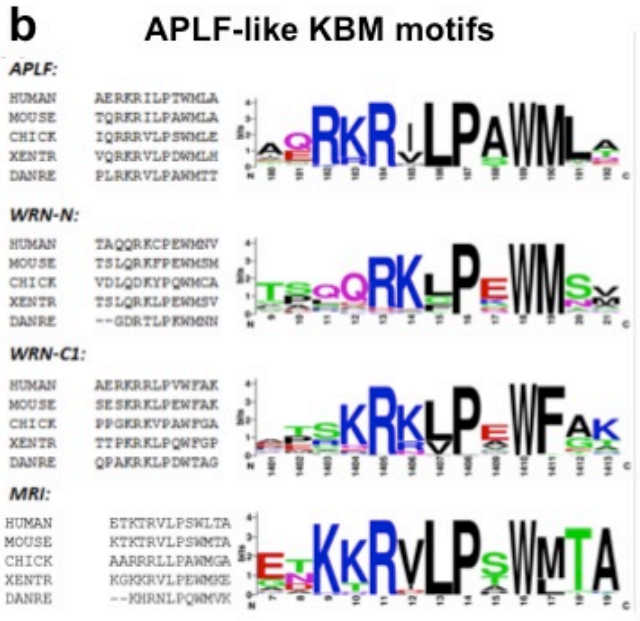
b
APLF-like KBM motifs
APLF:
HUMAN AERKRILPTWMLA
MOUSE TQRKRILPAWMLA
CHICK IQRRRVLPSWMLE
XENTR VQRKRVLPDWMLH
DANRE PLRKRVLPAWMTT
WRN-N:
HUMAN TAQQRKCPEWMNV
MOUSE TSLQRKFPEWMSM
CHICK VDLQDKYPQWMCA
XENTR TSLQRKLPEWMSV
DANRE --GDRTLPKWMNN
WRN-C1:
HUMAN AERKRRLPVWFAK
MOUSE SESKRKLPEWFAK
CHICK PPGKRKVPAWFGA
XENTR TTPKRKLPQWFGP
DANRE QPAKRKLPDWTAG
MRI:
HUMAN ETKTRVLPSWLTA
MOUSE KTKTRVLPSWMTA
CHICK AARRRLLPAWMGA
XENTR KGKKRVLPEWMKE
DANRE --KHRNLPQWMVK

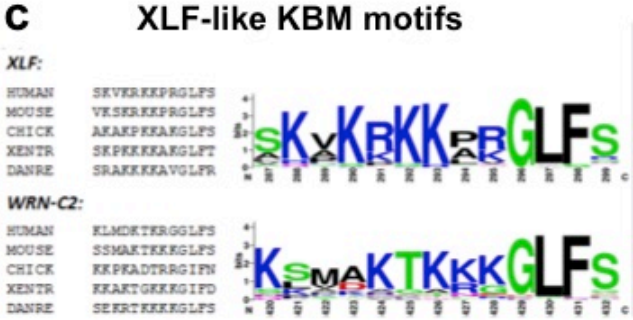
c
XLF-like KBM motifs
XLF:
HUMAN SKVKRKKPRGLFS
MOUSE VKSKRKKPRGLFS
CHICK AKAKPKKAKGLFS
XENTR SKPKKKKARGLFT
DANRE SRAKKKKAVGLPR
WRN-C2:
HUMAN KLMDKTKRGGLFS
MOUSE SSMAKTKKKGLFS
CHICK KKPRADTRRGIFN
XENTR KKAKTGKKKGIFD
DANRE SEKRTKKKKGLFS

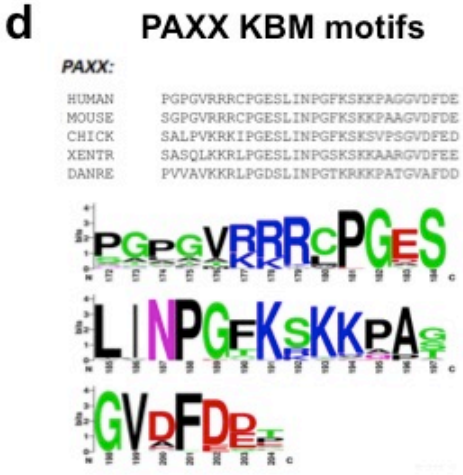
d
PAXX KBM motifs
PAXX:
HUMAN PGPGVRRRCPGESLINPGFKSKKPAGGVDFDE
MOUSE SGPGVRRRCPGESLINPGFKSKKPAAGVDFDE
CHICK SALPVKRKIPGESLINPGFKSKSVPSGVDFED
XENTR SASQLKKRLPGESLINPGSKSKKAARGVDFEE
DANRE PVVAVKKRLPGDSLINPGTKRKKPATGVAFDD

Supplementary Figure 1

Functions and conservation of KBMs.

(a) Scheme of the interactions between Ku70-Ku80 and the NHEJ factors containing an A-KBM (APLF, CYREN), an X-KBM (XLF) and both KBMs (WRN). The interaction of PAXX with Ku70 through its C-terminus is also represented. **(b-d)** Logo motif of the A-KBM, X-KBM and PAXX motifs obtained from multiple sequences alignment of these proteins as indicated (Crooks, G.E. *et al.*, WebLogo: a sequence logo generator. Genome Res 14, 1188-90 (2004)).

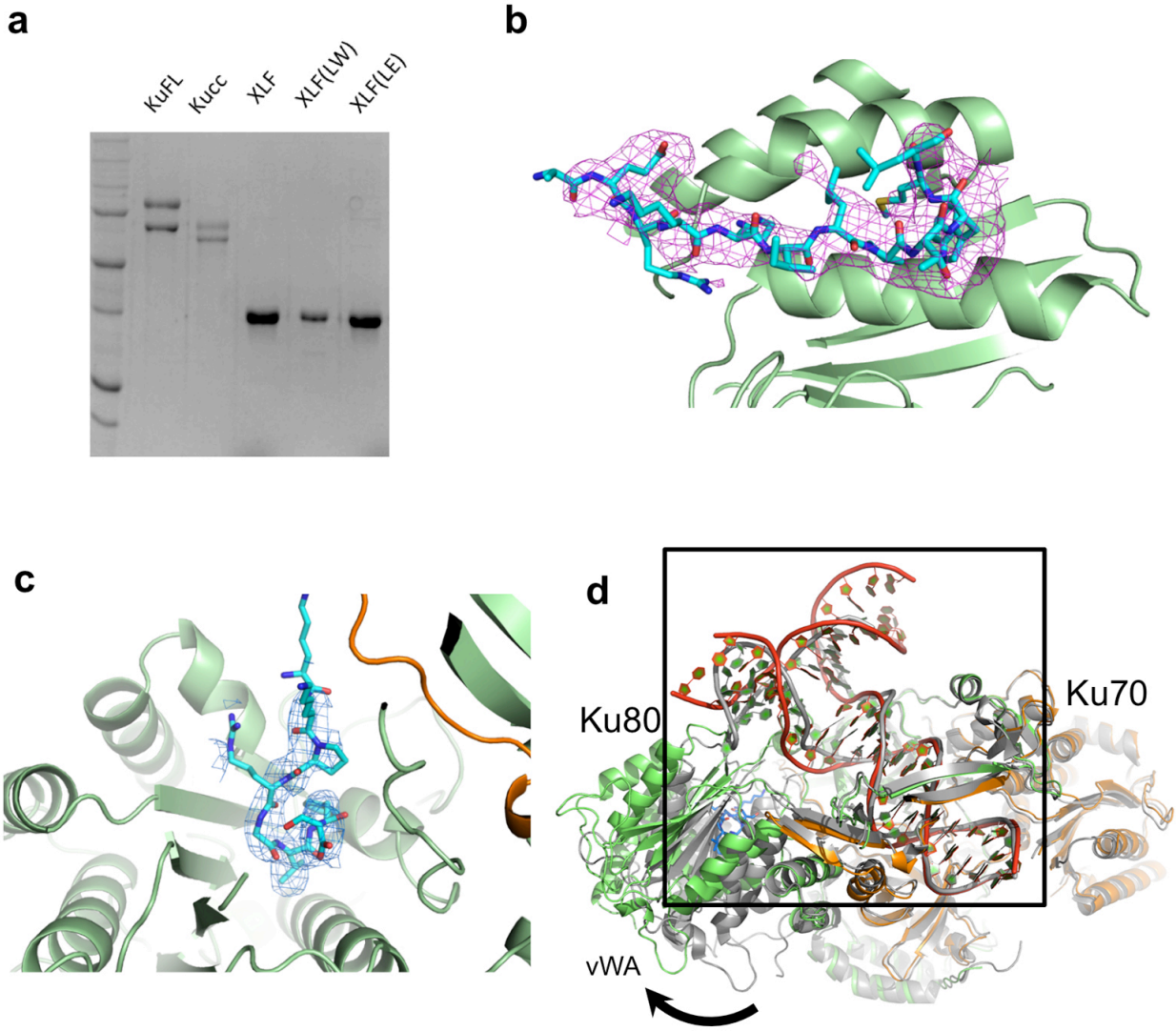
a
KuFL
Kucc
XLF
XLF(LW)
XLF(LE)
b
c
d
Ku80
Ku70
vWA
e
Time (min)
µcal/sec
KCal/Mole of Injectant
Molar Ratio
(C) Ku$_{FL}$ 12 µM
(S) pAPLF 120 µM
f
Time (min)
µcal/sec
kcal mol^{-1} of injectant
Molar Ratio
(C) Ku$_{FL}$ 16µM
(S) pXLF 160µM
g
Time (min)
µcal/sec
KCal/Mole of Injectant
Molar Ratio
(C) Ku$_{FL}$ 11 µM
(S) pXLF (LW) 95 µM

Supplementary Figure 2

Protein purification, structural and ITC data.

(a) SDS gel showing purified Ku and XLF proteins as indicated. FL: full-length; cc: C-terminal truncation. **(b)** Electron density of peptide pAPLF. **(c)** Electron density of peptide pXLF. (**c**) DNA interactions with Ku in presence of X-KBM of XLF. Ku70-Ku80-hDNA-X-KBM (colored) compared to Ku70/Ku80/hDNA (PDB 1JEY, grey). Front view of Ku70-Ku80-hDNA-X-KBM showing the major deviation of hDNA molecules because of the conformational change of Ku80. (**d-e**) ITC analyses: representative thermograms and isotherms of titration corresponding to selected measurements from Table 2, as indicated.

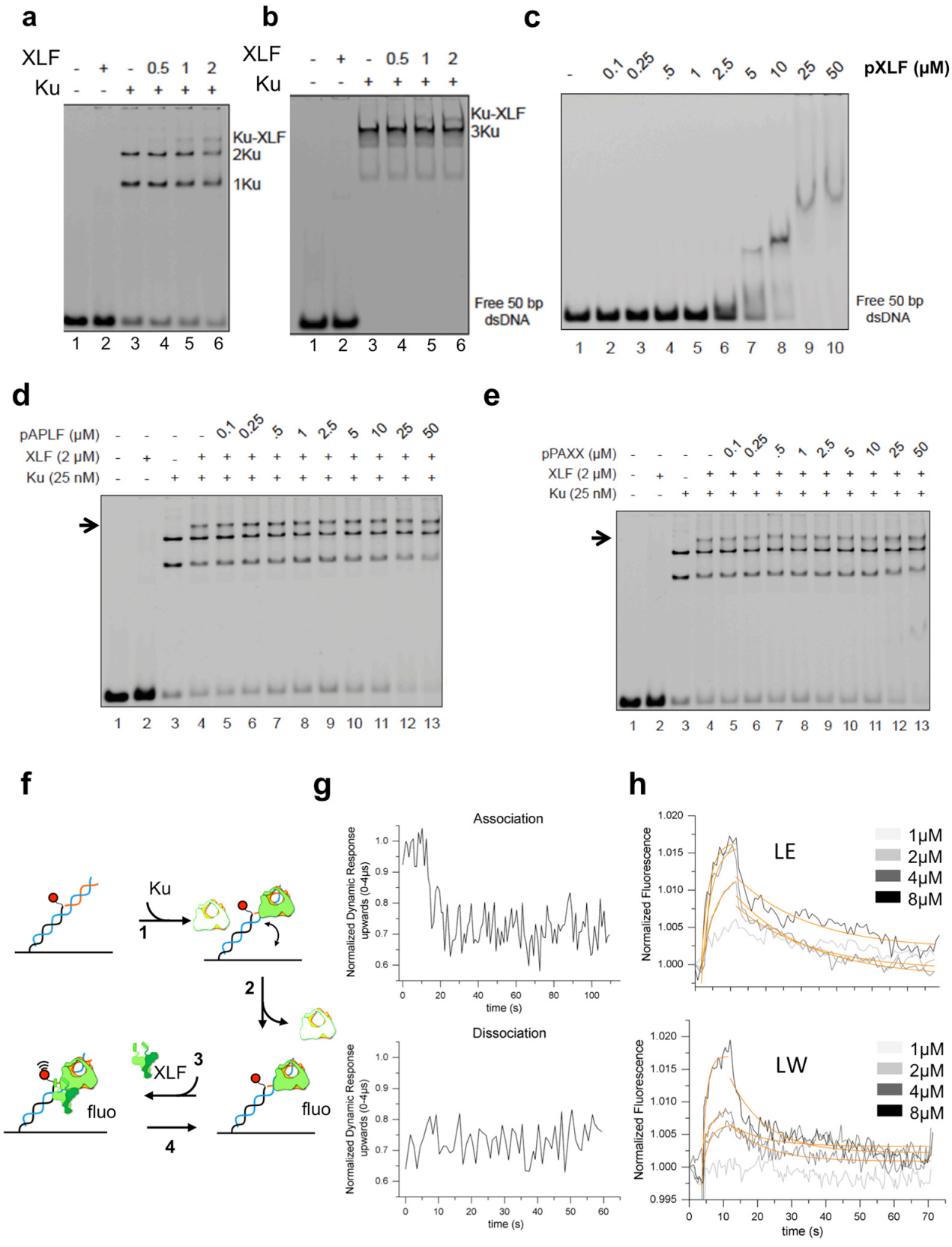
a
XLF
Ku
Ku-XLF
2Ku
1Ku
1 2 3 4 5 6
b
XLF
Ku
Ku-XLF
3Ku
Free 50 bp
dsDNA
1 2 3 4 5 6
c
pXLF (μM)
Free 50 bp
dsDNA
1 2 3 4 5 6 7 8 9 10
d
pAPLF (μM)
XLF (2 μM)
Ku (25 nM)
1 2 3 4 5 6 7 8 9 10 11 12 13
e
pPAXX (μM)
XLF (2 μM)
Ku (25 nM)
1 2 3 4 5 6 7 8 9 10 11 12 13
f
Ku
1
2
XLF
3
4
fluo
fluo
g
Association
Normalized Dynamic Response upwards (0-4μs)
time (s)
Dissociation
Normalized Dynamic Response upwards (0-4μs)
time (s)
h
LE
LW
1μM
2μM
4μM
8μM
Normalized Fluorescence
time (s)

Supplementary Figure 3

EMSA and switchSENSE data.

(a-e) EMSA analyses: (a, b) Gel shift assays with XLF and Ku at 20nM (a) or 200nM concentrations (b) in presence of a 50bp DNA with a FAM in 5'. **(c)** pXLF interaction with DNA as a control of the competition experiment in Figure 2e. **(d-e)** The pAPLF and PAXX Cter do not compete with the Ku-XLF complex. **(f-h) switchSENSE analyses: (f)** Scheme of the switchSENSE measurement flow: 1) Ku is bound to an 80bp nanolever with a fluorescent probe at position 48; 2) A washing step removes non-specifically bound Ku molecules; 3) XLF is then injected for real-time associations and dissociations at different concentrations followed by normalized changes in the fluorescence. **(g)** Binding kinetics of the Ku protein on the 80mer double-stranded DNA prior to the interaction with XLF, shown as changes in the dynamic response upwards (between 0 and 4µs). The dynamic response reflects the speed of the switching DNA, which decreases upon binding of the Ku analyte. The dissociation is represented only for one minute, to show that no dissociation of Ku from the DNA occurs while the XLF kinetics is measured. **(h)** Kinetic analyses of (LW) and (LE)XLF interactions. Solid grey lines represent raw data (from 1 to 8 µM; light grey to dark grey; averages of triplicates). Global fitting was performed, following a single-exponential function (solid orange lines) yielding kinetic rate constants; k_{ON} = 4.9 ± 0.5 10^{4} $M^{-1}s^{-1}$ and k_{OFF} = 4.8 ± 0.5 10^{-2} s^{-1} for XLF(LE) and k_{ON} = 1.9 ± 1.1 10^{5} $M^{-1}s^{-1}$and k_{OFF} = 8.4 ± 0.6 10^{-2} s^{-1} for XLF(LW).

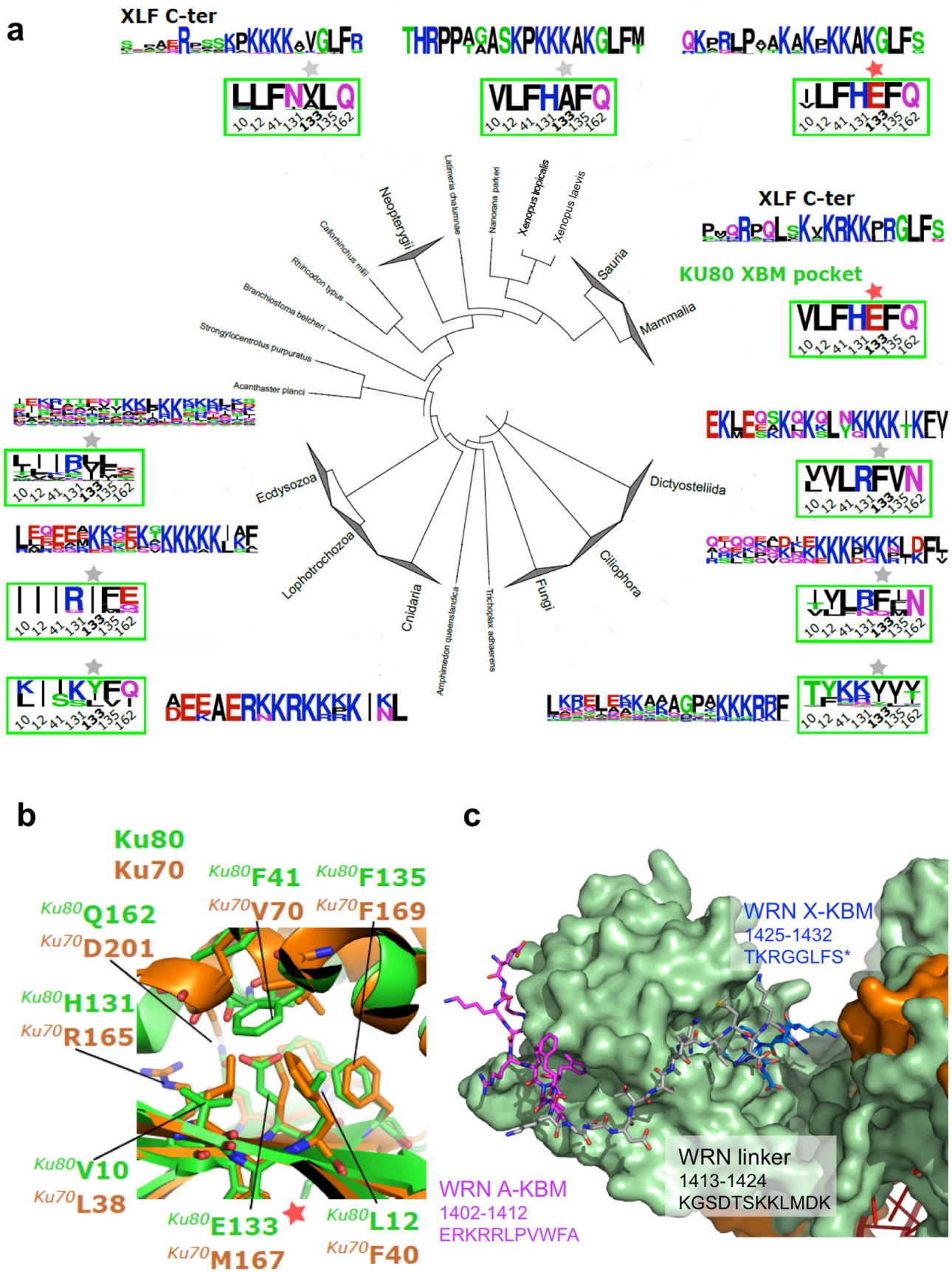
a
XLF C-ter
KU80 XBM pocket
Neopterygii
Latimeria chalumnae
Nanorana parkeri
Xenopus tropicalis
Xenopus laevis
Sauria
Mammalia
Callorhinchus milii
Rhincodon typus
Branchiostoma belcheri
Strongylocentrotus purpuratus
Acanthaster planci
Ecdysozoa
Lophotrochozoa
Cnidaria
Amphimedon queenslandica
Trichoplax adhaerens
Fungi
Ciliophora
Dictyosteliida
b
Ku80
Ku70
Ku80F41
Ku80F135
Ku80Q162
Ku70V70
Ku70F169
Ku70D201
Ku80H131
Ku70R165
Ku80V10
Ku70L38
Ku80E133
Ku80L12
Ku70M167
Ku70F40
c
WRN X-KBM
1425-1432
TKRGGLFS*
WRN linker
1413-1424
KGSDTSKKLMDK
WRN A-KBM
1402-1412
ERKRRLPVWFA

Supplementary Figure 4

Evolution of X-KBM binding site in Ku80, comparison with Ku70 and modelling of WRN C terminus binding.

(a) Variations among the sequence motifs observed for the C-terminal tail of XLF and for the seven positions of the Ku80 XBM pocket in various clades of the eukaryotic phylogenetic tree. 10 clades are represented summarizing the properties of 60 Mammalia, 36 Sauria, 31 Neopterygii, 62 Ecdysozoa, 9 Lophotrochozoa, 5 Cnidaria, 150 Fungi, 5 Ciliophora and 4 Dictyostellida sequences of XLF and Ku80. For each clade, web logos of the last 25 C-terminal amino-acids of XLF sequences are represented on top and the web logo of the X-KBM site positions is squared in green. A red star indicates the clades in which the position of Ku80 E133 was conserved as an acidic residue whereas a grey star points out that the acidic character of the residue was not maintained and was generally switched to a hydrophobic residue as observed in Ku70. **(b)** Superimposition of human Ku70 and Ku80 structures (PDB: 1JEQ) colored in orange and green, respectively, and focused on the region surrounding Ku80 E133 position in the X-KBM site. The red star points out the location of Ku80E133. Residues labelled and shown as sticks are the spatial neighbours of Ku80 E133. The side chain of Ku80 E133 is buried in the hydrophobic core of Ku80 and is not involved in any hydrogen bond or salt-bridge interaction resulting in a predicted pKa above 9.1 in the absence of XLF. **(c)** Molecular modelling of the interaction between Ku80 and the C-terminus of WRN containing an A-KBM in tandem with a X-KBM. The position of WRN motifs were deduced from the crystal structures presented here with APLF and XLF KBMs. The orientation of the KBMs and the size of the linker between WRN KBMs are compatible with a simultaneous binding of both WRN motifs to Ku80.

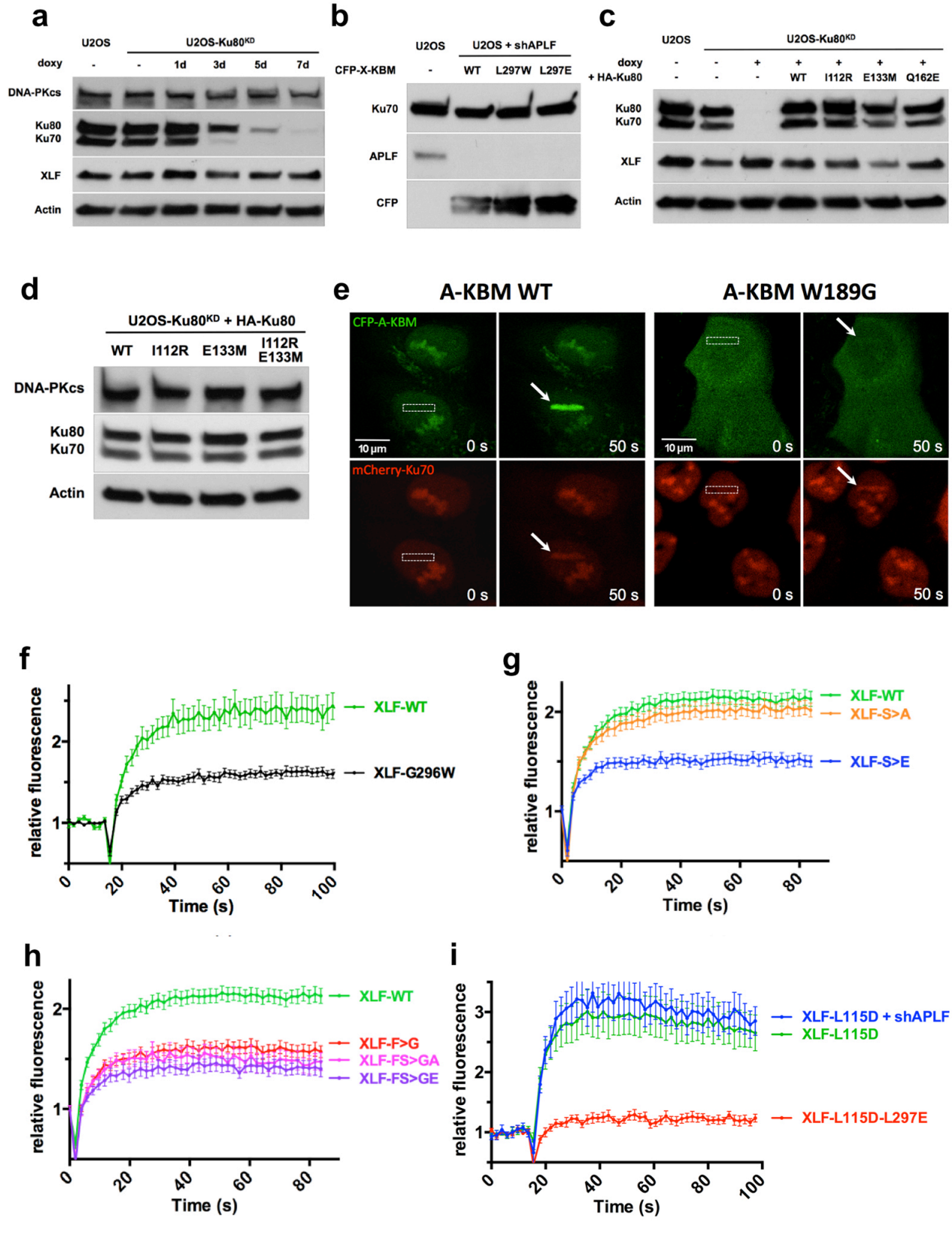
a
U2OS
U2OS-Ku80KD
doxy
-
-
1d
3d
5d
7d
DNA-PKcs
Ku80
Ku70
XLF
Actin
b
U2OS
U2OS + shAPLF
CFP-X-KBM
-
WT
L297W
L297E
Ku70
APLF
CFP
c
U2OS
U2OS-Ku80KD
doxy
+ HA-Ku80
WT
I112R
E133M
Q162E
Ku80
Ku70
XLF
Actin
d
U2OS-Ku80KD + HA-Ku80
WT
I112R
E133M
I112R
E133M
DNA-PKcs
Ku80
Ku70
Actin
e
A-KBM WT
A-KBM W189G
CFP-A-KBM
mCherry-Ku70
10 μm
0 s
50 s
f
relative fluorescence
Time (s)
XLF-WT
XLF-G296W
g
relative fluorescence
Time (s)
XLF-WT
XLF-S>A
XLF-S>E
h
relative fluorescence
Time (s)
XLF-WT
XLF-F>G
XLF-FS>GA
XLF-FS>GE
i
relative fluorescence
Time (s)
XLF-L115D + shAPLF
XLF-L115D
XLF-L115D-L297E

Supplementary Figure 5

Western blotting and life cell imaging data**.**

(a-d) Western blot of U2OS cell extracts. **(a)** Whole cell extracts of U2OS shKu80 (U2OS-Ku80^{KD}) cells treated with doxycyclin for the indicated time were denatured and separated on 10% SDS-PAGE gel followed by electrotransfer on membrane. The membranes were blotted with the antibodies as indicated. **(b)** Whole cell extracts of U2OS shAPLF cells expressing WT or mutant CFP-X-KBM as indicated were processed as in (a). **(c)** Whole cell extracts of U2OS-Ku80^{KD} cells treated with doxycyclin for 7 days and expressing WT or mutant HA-Ku80 as indicated were processed as in (a). **(d)** Whole cell extracts of U2OS-Ku80^{KD} cells treated with doxycyclin for 7 days and expressing WT or mutant HA-Ku80 as indicated were processed as in (a). Uncropped blot images are shown in Supplementary Data Set 1. **(e)** Wild-type (WT) or mutant CFP-(A-KBM) and mCherry-Ku70 simultaneous behaviour after 800 nm pulsed-laser nuclear micro-irradiation assessed in U2OS cells by live cell-imaging at 0 s and 50 s post-irradiation. The white rectangle and arrows mark irradiated areas. **(f-h)** Dynamics of wild-type (WT) and mutant CFP-tagged full-length XLF at laser-damaged sites in BuS cells. Images were obtained at 1.94 s intervals and fluorescence intensities at the damage sites and in undamaged area were quantified. Mean values of the relative fluorescence with SEM were calculated from 20 independent measurements for each of WT and G296W XLF in (f), from 45, 40 and 20 independent measurements for each of WT, S299A and S299E XLF in (g) and from 45, 36, 20 and 20 independent measurements for each of WT, F298G, F298G/S299A, and F298G/S299E XLF in (h), respectively. *p* values at last time point: (f) WT vs G296W $p<0.0001$; (g) WT vs S>A $p=0.2785$; WT vs S>E $p<0.0001$. (h) WT vs F>G $p<0.0001$; WT vs FS>GA $p<0.0001$; WT vs FS>GE $p<0.0001$. **(i)** Dynamics of L115D and L115D/L233E CFP-tagged full-length mutant XLF at laser-damaged sites in BuS cells as in (f). Mean values of the relative fluorescence with SEM were calculated from 11 independent measurements for each of L115D±shAPLF and L115D/L233E XLF conditions. *p* values at last time point: L115D vs L115D±shAPLF $p=0.6113$; L115D vs L115D/L233E $p=0.0002$.

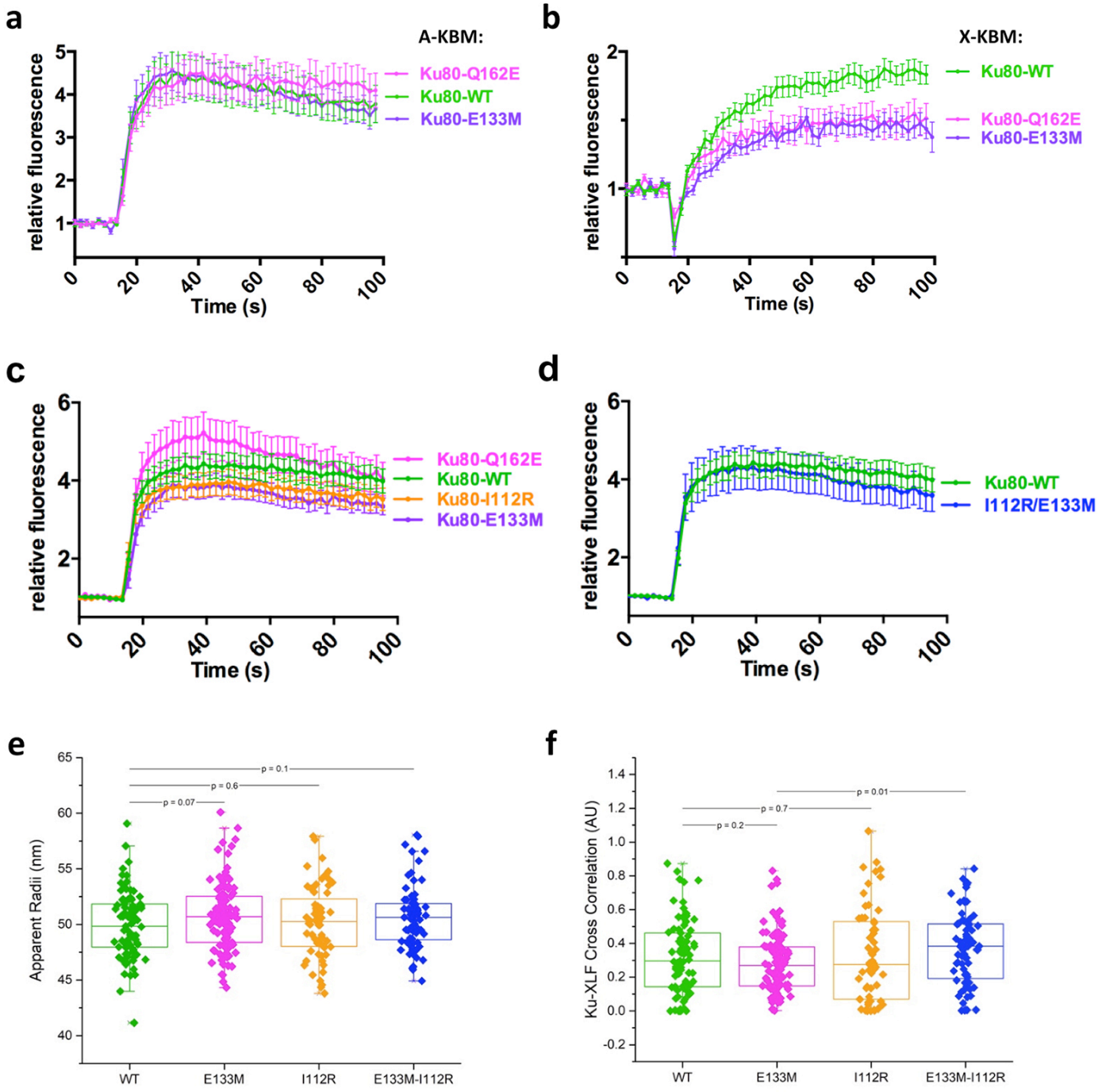

Supplementary Figure 6

Life cell imaging, super resolution and DNA repair assays data.

(a-b) Dynamics of CFP-(A-KBM) (a) and (X-KBM) (b) at laser damaged sites in U2OS cells expressing wild-type (WT), E133M or Q162E mutant Ku80 as in Figure 3 b). Mean values of the relative fluorescence with SEM were calculated from 20, 23 and 22 independent measurements for A-KBM with WT, E133M or Q162E mutant Ku80 in (a) and from 48, 29 and 29 independent measurements for X-KBM with WT, E133M or Q162E mutant Ku80 in (b), respectively. *p* values at last time point: (a) WT vs E133M

p=0.831; WT vs Q162E *p*=0.59519; (b) WT vs E133M *p*=0.0003; WT vs Q162E *p*=0.0111. **(c-d)** Dynamics of wild-type (WT) and mutant CFP-Ku80 at laser damaged sites in U2OS cells. Mean values of the relative fluorescence with SEM were calculated from 25, 24, 20 and 15 independent measurements for WT, I112R, E133M and Q162E mutant Ku80 in (c) and from 25 and 26 independent measurements for WT or I112R/E133M mutant Ku80 in (d), respectively. *p* values at last time point: (c) WT vs Q162E =0.9252; WT vs I112R *p*=0.2734; WT vs E133M *p*=0.1101. (d) WT vs I112R-E1333M *p*=0.5362. (**e-f**) Analysis of XLF foci in U2OS cells by super-resolution. (e) Statistics of XLF foci size: each plot represents the average XLF foci size (indicated as radius translated from the correlation radius) in one nucleus. Box's height displays the standard deviation with the mean value labelled in the middle. 87, 110, 64, and 79 nuclei were taken in account for WT, E133M, I112R, and E133M-I112R double-mutant, respectively. The *p*-values were obtained by the t-test; (f) Statistics of the Cross-Pair-Correlation between Ku and XLF: Ku and XLF were stained with antibodies labelled by different fluorophores (Alexa488 conjugated rabbit anti-Ku80, abcam198586, Alexa647 conjugated goat anti-mouse secondary + Mouse anti-XLF, NBP2-03275), and dual-colour super-resolution imaging was performed to examine the cross-correlation between Ku and XLF foci within each nucleus. Each plot represents the cross-correlation amplitude calculated across one nucleus. Box's height displays the standard deviation with the mean value labelled in the middle. 83, 107, 57, and 72 nuclei were taken in account for WT, E133M, I112R, and E133M-I112R mutants respectively. The *p*-value were obtained by the t-test.

Expression vectors

All lentiviral vectors derived from pLVTHM (Addgene plasmid #12247) and pLV-tTR- KRAB-Red (Addgene plasmid #12250) plasmids. Both were gifts from Didier Trono [1].

The pLVTHM2 vector was obtained by digesting pLVTHM with PmeI/SpeI and inserting the PBXS linker (i.e. preannealed PBXS-F/PBXS-R pair of oligonucleotides) in order to remove the GFP coding sequence. To generate lentiviral vectors for conditional expression of shRNA, pLVTHM2 was digested with MluI/ClaI and the following pairs of preannealed oligonucleotides were inserted by ligation: shKu80-F/shKu80-R (target sequence designed by Denis Biard, CEA-DSV, France, personal communication) or shAPLF- F/shAPLF-R (target sequence from [2]) to knockdown the expression of Ku80 or APLF, respectively.

The pLV-tTR-KRAB vector was obtained from pLV-tTR-KRAB-Red by replacing the DsRed coding sequence by the XBES linker at XmaI/SpeI restriction sites.

The pLV-Red vector derived from pLV-tTR-KRAB-Red by replacing the tTR-KRAB coding sequence by the PEKBBMX linker at PmeI/XmaI restriction sites.

The pLV3 vector derived from pLV-tTR-KRAB-Red through the following modifications: first, the NsiI/Kpn2I fragment was replaced by the nPNk linker. The tTR- KRAB coding sequence was then removed by PmeI/XmaI digestion and replaced by the PEKBBMX linker. Finally, the IRES-DsRed fragment was removed by PmeI/SpeI digestion and replaced by the PKXMBBES linker.

To express ECFP-tagged A-KBM (APLF P177 to E193) or X-KBM (XLF S287 to S299) motifs, the A-KBM linker or X-KBM linker, respectively, was inserted into the Acc65I/BamHI restriction sites of the pECFP-C1 plasmid (Clontech) and the AgeI/BamHI fragment (ECFP-A-KBM or ECFP-X-KBM) was subcloned into the Kpn2I/BamHI restriction sites of pLV3. The ECFP-tagged A-KBM-W189G, X-KBM-L297W and X-KBM-L297E expressing vectors were obtained by amplifying by PCR the corresponding cDNAs using the pECFP-A-KBM or pECFP-X-KBM plasmid as a template, as well as CMV-F as forward primer and Bam-A-KBM-W189G-R, XLF-L297W-Bam-R or XLF-L297E-Bam-R as reverse primer, respectively. The PCR fragments were digested with AgeI/BamHI and inserted into Kpn2I/BamHI restriction sites of pLV3.

To express full-length ECFP-tagged XLF protein, human XLF cDNA (a gift from Jean-Pierre de Villartay, Institut Imagine, Paris, France) was amplified by PCR using the XLF-Hind-F and XLF-Bam-R primers. The resulting PCR fragment was digested with HindIII/BamHI and inserted into pECFP-C1. The ECFP-XLF coding fragment was then excised with AgeI/BamHI and inserted into pLV3 at Kpn2I/BamHI restriction sites. ECFP-XLF-L297W, -L297E, -F298G, -S299A, -S299E, -F298G-S299A, and -F298G-S299E mutants were expressed by PCR amplification of the corresponding XLF coding sequences using the pECFP-XLF vector as a template, Kpn2-MCS-F as forward primer, and XLF-L297W-Bam-R, XLF-L297E-Bam-R, XLF-F298G-Bam-R, XLF-S299A-Bam-R, XLF-S299E-Bam-R, XLF-FS298GA-Bam-R, or XLF-FS298GE-Bam-R, as reverse primer, respectively. The resulting fragments were digested with Kpn2I/BamHI and inserted into pLV3-ECFP-XLF to replace the XLF wild-type coding sequence. The XLF-L115D coding sequence was obtained by overlapping PCR mutagenesis on pLV3-ECFP-XLF template using ECFP-Cter-F and XLF-Bam-R oligos as outer primers, and XLF-L115D-F and XLF-L115D-R as mutated inner primers. The PCR product (XLF-L115D) was then digested with Kpn2I/BamHI and inserted into pLV3-ECFP-XLF to replace the XLF-WT coding sequence. The XLF-L115D-L297E double mutant coding sequence was obtained as above, except that the XLF-Bam-R outer primer was replaced by XLF-L297E-Bam-R.

Lentiviral vectors expressing untagged full-length XLF proteins (WT, L297W or L297E) were obtained by subcloning Kpn2I/BamHI fragments from the respective pLV3-ECFP-XLF into the pLV-Red vector.

The ECFP-XRCC4 expressing vector was obtained by excision of a Kpn2I/BamHI fragment containing the XRCC4 coding sequence from the pEGFP-C1-FLAG-XRCC4 plasmid (gift from Steve Jackson (Addgene #46959), [3]). The resulting fragment was inserted into pLV3-ECFP-XLF to replace the XLF coding sequence.

To obtain shRNA-resistant human Ku80 expression vector, HA-Ku80 coding sequence was amplified by overlapping PCR from pICE-Puro-HA-Ku80 (a kind gift from Sébastien Britton, IPBS, Toulouse, France) with Kpn2-HA-F and pICE-Xba-R as outer primers, and Ku80-shRes-F and Ku80-shRes-R as inner primers that introduce silent mutations in the shRNA target sequence. The resulting fragment was then inserted into pLV3 after digestion with Kpn2I/MluI. The Ku80-L112R expressing pLV3 vector was constructed by overlapping PCR from pLV3-HA-Ku80-shR using pLV-F and pLV-R oligonucleotides as outer primers and Ku80-L112R-F and Ku80-L112R-R as mutated inner primers. The PCR product was then digested with Kpn2I/MluI and inserted into pLV3. Other Ku80 single mutant constructs

(E133M and Q162E) were obtained similarly by using the corresponding pairs of inner primers (Ku80-E133M-F/Ku80-E133M-R and Ku80-Q162E-F/Ku80-Q162E-R, respectively). The pLV3-HA-Ku80-shR-L112R-E133M double mutant expressing vector was obtained as above for the E133M single mutant construct, except that pLV3-HA-Ku80-shR-I112R was used as a template for PCR reactions.

Expression vectors for ECFP-tagged WT or mutants Ku80 were obtained by amplifying the ECFP coding sequence by PCR from the pECFP-C1 plasmid with the Pme-Koz-ECFP-F and pme-CFP-80-R primers. The PCR fragment was then inserted at the PmeI restriction site in the various pLV3-HA-Ku80-shR plasmids by use of the Hot-Fusion strategy [4].

To generate pLV3-mCherry-FLAG-Ku70 vector allowing expression of an mCherry-tagged Ku70 protein, the FLAG-Ku70 coding sequence was amplified by PCR using Kpn2-FLAG-F and Mlu-Ku70-R primers, digested with Kpn2I/MluI and cloned into pLV3. The mCherry coding sequence was then inserted at the PmeI restriction site by Hot-Fusion cloning [5] following PCR amplification using Pme-Koz-ECFP-F and Kpn2-pme-mCh-R primers and the pmCherry-C1-3NLS plasmid as a template (gift from Dyche Mullins (Addgene #58476), [6]).

The pLV3-Tet-RFP-ISceI-GRLBD lentiviral vector for conditional expression of I-SceI was prepared as follows : pLV3 was first modified by inserting at the PacI restriction site the Tet-Pac-F/Tet-Pac-R pre-annealed linker which contains two tetracyclin operator DNA elements. The resulting pLV3-Tet plasmid was then digested by Kpn2I/BamHI to receive the AgeI/BamHI fragment from the pISceI-GR-RFP plasmid (gift from Tom Misteli (Addgene #17654), [7]) which contains the coding sequence of DsRed-ISceI-GRLBD.

All oligonucleotides were purchased from Eurofins Genomics (Ebersberg, Germany). Restriction and modifying enzymes (Phusion and T4 DNA Ligase) were from ThermoFisher Scientific (Illkirch, France). All constructs were checked by sequencing (Eurofins Genomics).

Oligonucleotides used as linkers (alphabetical order; sequences 5' to 3')

A-KBM-F	GTACC CCA ATC CTT GCC GAG AGG AAA AGA ATC CTT CCA ACT TGG ATG TTA GCA GAA TAG
A-KBM-R	GATCCTA TTC TGC TAA CAT CCA AGT TGG AAG GAT TCT TTT CCT CTC GGC AAG GAT TGG G
nPNk-F	CTCCATCGATCGCCATGGTGA
nPNk-R	CCGGTCACCATGGCGATCGATGGAGTGCA

PBXS-F	AAAC CGTACG GATATC T CCCGGG TC A
PBXS-R	CTAGT GA CCCGGG A GATATC CGTACG GTTT
PEKBBMX-F	AAACTACGGGATC GAATTC CTCGCT TCCGGA CTTCGT GGATCC ACTCTC CGTACG ACTGCT ACGCGT ACTTCAC
PEKBBMX-R	CCGGGTGAAGT ACGCGT AGCAGT CGTACG GAGAGT GGATCC ACGAAG TCCGGA AGCGAG GAATTC GATCCCGTAGTTT
PKXMBBES-F	AAACTACGG GATC TCCGGA CACCTT CCCGGG TCACTC ACGCGT CTCATT GGATCC CGTACG GAATTC A
PKXMBBES-R	CTAGT GAATTC CGTACG GGATCC AATGAG ACGCGT GAGTGA CCCGGG AAGGTG TCCGGA GATC CCGTAGTTT
shAPLF-F	CGCGTCCCC GAA GAA ATC TGC AAA GAT A TTCAAGAGA T ATC TTT GCA GAT TTC TTC TTTTTGGAAAT
shAPLF-R	CGATTTCCAAAAA GAA GAA ATC TGC AAA GAT A TCTCTTGAA T ATC TTT GCA GAT TTC TTC GGGGA
shKu80-F	CGCGTCCCC G AAC AAG GAT GAG ATT GCT TTCAAGAGA AGC AAT CTC ATC CTT GTT C TTTTTGGAAAT
shKu80-R	CGATTTCCAAAAA G AAC AAG GAT GAG ATT GCT TCTCTTGAA AGC AAT CTC ATC CTT GTT C GGGGA
TetO-Pac-F	TCCCTATCAGTGATAGAGATCTCCCTATCAGTGATAGAGAAT
TetO-Pac-R	TCTCTATCACTGATAGGGAGATCTCTATCACTGATAGGGAAT
XBES-F	CCGGG GGATCC CTCGAG GAATTC A
XBES-R	CTAGT GAATTC CTCGAG GGATCC C
X-KBM-F	GTACC TCA AAG GTC AAG AGG AAG AAG CCA AGG GGT CTC TTC AGT TAG
X-KBM-R	GATCCTA ACT GAA GAG ACC CCT TGG CTT CTT CCT CTT GAC CTT TGA G

Oligonucleotides used as PCR primers (alphabetical order; sequences 5' to 3')

Bam-A-KBM-W189G-R	CGTACGGGATC CTA TTC TGC TAA CAT CCC AGT TGG AAG GAT TCT TTT CCT C
CMV-F	GTAGGCGTGTACGGTGGGAGG
ECFP-Cter-F	C ATG GTC CTG CTG GAG TTC GTG
Kpn2-HA-F	CTCTGC TCCGGA GCCACC ATG TAC CCC TAC GAT GTG C
Kpn2-FLAG-F	CTCTCGTCCGGAGCCGCACC ATG GAC TAC AAG GAT G
Kpn2-MCS-AKF-F	CTCGCTTCCGGACTCAGATCTCGAGCTC
Kpn2-pme-mCh-R	GGTGCGGCTCCGGAGATCCCGTAGTTTGGACTTGTACAGCTCGTCCATGCCG
Ku80-E133M-F	GAG GCA TAT TAT GAT ATT CAC TGA CCT CAG CAG CCG ATT C
Ku80-E133M-R	GGT CAG TGA ATA TCA TAA TAT GCC TCT TCT CAA ACT TCT TTC CTA TTG
Ku80-I112R-F	C TTC CTG GAT GCA CTA AGA GTG AGC ATG GAT GTG ATT CAA C
Ku80-I112R-R	G AAT CAC ATC CAT GCT CAC TCT TAG TGC ATC CAG GAA GTC
Ku80-Q162E-F	CAT CTC CCT GGA ATT CTT CTT GCC TTT CTC ACT TGG C

Ku80-Q162E-R	GGC AAG AAG AAT TCC AGG GAG ATG TCA CAT TTC TTC AAG C
Ku80-shRes-F	GCT GAA AAT AAA GAC GAA ATC GCC TTA GTC CTG TTT GGT ACA GAT GGC
Ku80-shRes-R	GAC TAA GGC GAT TTC GTC TTT ATT TTC AGC AAA CAC CTG TCG CTG TAC
Mlu-Ku70-R	CTCTGCACGCG TCA GTC CTG GAA GTG CTT GGT GAG GGC
pICE-Xba-R	CAGCGGGTTTA TCTAGA CTGCAG ACGCGT GC
pLV-F	CCGATCACGAGACTAGCCTCGAGG
pLV-R	CCAGTCAATCTTTCACAAATTTTGTAATCCAGAGG
pme-CFP-80-R	CATGGTGGCTCCGGAGATCCCGTAGTTTGACTTGTACAGCTCGTCCATGCCG
Pme-Koz-CFP-F	CGATCACGAGACTAGCCTCGAGGTTTAAACGCCGCCACCATGGTGAGCAAGG GC
XLF-Bam-R	CTCTC GGATC CTA ACT GAA GAG ACC CCT TGG CTT CTT CCT CTT GAC C
XLF-F298G-Bam-R	CTCTC GGATC CTA ACT GCC GAG ACC CCT TGG CTT CTT CCT CTT GAC C
XLF-FS298GA-Bam-R	CTCTCGGATC CTA AGC GCC GAG ACC CCT TGG CTT CTT CCT CTT GAC C
XLF-FS298GE-Bam-R	CTCTCGGATC CTA CTC GCC GAG ACC CCT TGG CTT CTT CCT CTT GAC C
XLF-Hind-F	CTCTCAAGCTTCCGCCACC ATG GAA GAA CTG GAG CAA GGC CTG
XLF-L115D-F	G CGA AGT GAG CTC TCT GGC GAC CCC TTC TAT TGG AAT TTC C
XLF-L115D-R	G GAA ATT CCA ATA GAA GGG GTC GCC AGA GAG CTC ACT TCG C
XLF-L297E-Bam-R	CTCTC GGATC CTA ACT GAA CTC ACC CCT TGG CTT CTT CCT CTT GAC C
XLF-L297W-Bam-R	CTCTC GGATC CTA ACT GAA CCA ACC CCT TGG CTT CTT CCT CTT GAC C
XLF-S299A-Bam-R	CTCTCGGATC CTA AGC GAA GAG ACC CCT TGG CTT CTT CCT CTT GAC C
XLF-S299E-Bam-R	CTCTCGGATC CTA CTC GAA GAG ACC CCT TGG CTT CTT CCT CTT GAC C

References

1. Wiznerowicz, M. & Trono, D. Conditional suppression of cellular genes: lentivirus vector-mediated drug-inducible RNA interference. *J Virol* **77**, 8957-61 (2003).
2. Iles, N., Rulten, S., El-Khamisy, S.F. & Caldecott, K.W. APLF (C2orf13) is a novel human protein involved in the cellular response to chromosomal DNA strand breaks. *Mol Cell Biol* **27**, 3793-803 (2007).
3. Britton, S., Coates, J. & Jackson, S.P. A new method for high-resolution imaging of Ku foci to decipher mechanisms of DNA double-strand break repair. *J Cell Biol* **202**, 579-95 (2013).
4. Fu, C., Donovan, W.P., Shikapwashya-Hasser, O., Ye, X. & Cole, R.H. Hot Fusion: an efficient method to clone multiple DNA fragments as well as inverted repeats without ligase. *PLoS ONE* **9**, e115318 (2014).

5. Frit, P., Barboule, N., Yuan, Y., Gomez, D. & Calsou, P. Alternative end-joining pathway(s): Bricolage at DNA breaks. *DNA Repair (Amst)* **17**, 81-97 (2014).
6. Belin, B.J., Lee, T. & Mullins, R.D. DNA damage induces nuclear actin filament assembly by Formin -2 and Spire-(1/2) that promotes efficient DNA repair. [corrected]. *Elife* **4**, e07735 (2015).
7. Soutoglou, E. et al. Positional stability of single double-strand breaks in mammalian cells. *Nat Cell Biol* **9**, 675-82. (2007).